Available online at www.sciencedirect.com
ScienceDirect
Journal of Hazardous Materials 143 (2007) 354–361
Journal of Hazardous Materials
www.elsevier.com/locate/jhazmat

Equilibrium isotherm modeling of cesium adsorption onto magnetic materials

R.R. Sheha *, E. Metwally

Nuclear Chemistry Department, Hot Laboratory Centre, Atomic Energy Authority, P.O. 13759, Cairo, Egypt

Received 18 July 2006; received in revised form 12 September 2006; accepted 13 September 2006
Available online 22 September 2006

Abstract

The present work investigates the adsorptive interactions of Cs ions with natural magnetite and synthesized iron ferrite in aqueous medium. The applied adsorbents were characterized by FTIR and DTA/TGA analyses. Batch adsorption studies were performed to evaluate the influences of various experimental parameters like initial pH, contact time and initial concentration on the removal of Cs. The adsorption is strongly dependent on pH of the medium where the removal efficiency increases as the pH turns to alkaline range. The process was very fast initially and maximum adsorption was attained within 60 min of contact. The adsorption process follows a pseudo-second order kinetics with rate constant amounted to 76.83×10^4 and 18.75×10^4 g mg^{-1} h^{-1} with ferrite and magnetite. The presence of interfering cations seriously decreases the extent of Cs adsorption. The equilibrium data of Cs adsorption on both adsorbents were analyzed using the Freundlich, Langmuir, Temkin, Dubinin–Radushkevich and Redlich–Peterson isotherm models. The different isotherms constants were determined from the linearized form of their equations and used to characterize Cs distribution on adsorbent surfaces and provide adopted information about the affinity of the adsorbents towards Cs ions. The values of Langmuir separation factor indicate a favorable Cs adsorption. The apparent free energies from the Dubinin–Radushkevich are 32.29 and 27.51 kJ mol^{-1} for Cs adsorption onto iron ferrite and magnetite, respectively.

Keywords: Cesium; Adsorption; Ferrite; Magnetite; Isotherm models

1. Introduction

Radioactive waste is an inevitable residue from the use of radioactive materials in industry and medicine sector as well as from research and nuclear establishments. The management and disposal of such waste is, therefore, an issue relevant to almost all countries. The ever increasing pressure to reduce the release of radioactive and other toxic substances into the environment requires constant improvement/upgrading of processes and technologies for treatment and conditioning of liquid radioactive waste. In the aspect of radiological safety, cesium, cobalt and strontium are major radioactive isotopes because of their relatively long half-lives or high concentrations in the liquid wastes. ^{137}Cs is an important radionuclide has long half life ($t_{1/2}$ = 30.17 years) and represents a serious radiological hazard because, as an alkaline element, it exists as ionic forms and is easily assimilable by living organisms [1].

Treatment of liquid radioactive waste quite often involves the application of several steps such as precipitation, sorption, membrane separation and ion exchange to meet the requirements both for the release of decontaminated effluents into the environment and the conditioning of waste concentrates for disposal [2,3]. Ion exchange is one of the most important methods for the selective adsorption and safe storage of ^{137}Cs. The organic resins, selective towards cesium, are easily decomposed when exposed to highly ionizing radiation therefore application of inorganic ion exchangers is preferred. This is because they have several superior qualities required for the treatment of nuclear waste solutions, compared to organic resins, such as their higher thermal stability, resistance to ionizing radiation and good compatibility with the final waste forms [4–6]. The metal oxides are a group of inorganic ion exchangers that have been investigated extensively for application in nuclear waste treatment [7].

Ferrite is a metal oxide has common features with conventional inorganic adsorbents that are likely to be used in radioactive waste treatment and disposal such as high radiological resistance and more compatibility with ultimate immobilization

* Corresponding author. Tel.: +20 10 529 15 48.
E-mail address: rsheha68@yahoo.com (R.R. Sheha).

0304-3894/$ – see front matter © 2006 Elsevier B.V. All rights reserved.
doi:10.1016/j.jhazmat.2006.09.041

matrices [8]. It is a ferromagnetic mixed valence iron oxide material which has the structure of cubic close packed and inverse spinel [9]. In addition, ferrite has high removal capacity towards heavy metal, transition elements and some important radionuclides and shows paramagnetic properties implying the possibility of magnetic control of the conditioning process [10–12].

In the present study, a simple neutralization method was used to prepare iron ferrite. The surface characteristics of the synthesized ferrite particles and natural magnetite were characterized by Fourier transform infrared (FTIR) spectroscopy and the thermal stability was confirmed by thermogravimetric analysis (TGA) and differential thermal analysis (DTA). The work aims to investigate the quantitative removal of Cs from liquid radioactive wastes using synthesized iron ferrite and natural magnetite under different operating conditions. The specific objective of this research was to model the equilibrium sorption data using different isotherm models.

2. Experimental

2.1. Chemicals and reagents

All chemicals and reagents used in this work were of analytical grade purity and used without further purification. The radioactive tracer ^{134}Cs was locally prepared by neutron irradiation. In this concern, a suitable weight of target materials was wrapped in aluminum foil and irradiated in the Egyptian second research reactor. After cooling, the sample was dissolved in appreciate solvent, evaporated to dryness and redissolved in double distilled water. The radionuclide activity was γ-radiometrically assayed using a well type NaI scintillation crystal connected to a single channel analyzer model Nucleas 550.

2.2. Preparation of ferrite

Iron ferrite was prepared by coprecipitating Fe^{2+} and Fe^{3+} ions by NaOH solution and treating under hydrothermal conditions [13,14]. About 100 mL of 0.25 M ferrous sulfate ($FeSO_4{\cdot}7H_2O$), as Fe^{2+} source, were added to a same volume of 0.5 M ferric nitrate ($Fe(NO_3)_3{\cdot}9H_2O$), as Fe^{3+} source, in a molar concentration ratio of 1:2 for iron ions. Chemical precipitation was achieved at 25 °C under vigorous stirring by adding 0.5 M NaOH solution till pH matched the value of 10.5. The precipitate was heated at 80 °C for 30 min, washed several times with bi-distilled water and finally dried in an air oven at 70 °C.

2.3. Instrumentation

The applied adsorbents were thermally characterized by TA-60WS Shimadzu Thermal Analysis and by FTIR analysis using a FT BOMEN-Michelson IR Spectrometer. The specific surface area was measured by the BET method using a Pore Size Micrometric-9320 model, USA. MA-235 digital pH meter (Mettler Toledo, UK) was used for pH measurements. A SBS-30 thermostated water bath shaker (from Stuart Scientific, UK) was used for batch equilibration experiments.

2.4. Adsorption procedure

Adsorption experiments were performed, using batch technique, by equilibrating 0.1 g of the magnetic adsorbent with a certain volume of solutions traced with a prefixed initial activity of ^{134}Cs in sealed glass bottles. The samples were shaken at 23 ± 1 °C and aliquots were taken at appreciate time intervals as necessary, centrifuged and radionuclides activity was γ-radiometrically assayed. The pH values were adjusted with 0.1 M HCl and/or 0.1 M NaOH solutions. In clarifying their effect as competing multivalent cations on adsorption of cesium, different concentrations in the range 0.05–0.4 M of the salts NaCl, $MgCl_2{\cdot}6H_2O$ and $AlCl_3$ were added to a set of traced aqueous solutions and equilibrated with the applied adsorbents. After equilibrium, samples were centrifuged and aliquots were subjected to γ-assay. The adsorption percentages (Ads.%) and distribution coefficient (K_d, mL g^{-1}) were calculated using the equations:

$$\text{Ads.}(\%) = \frac{A_0 - A_e}{A_0} \times 100 \quad (1)$$

$$K_d = \frac{A_0 - A_e}{A_0}\frac{V}{m} \quad (2)$$

where A_0 and A_e are the initial and equilibrium activities of Cs in aqueous solution, V the aqueous volume (mL) and m is the adsorbent weight (g).

2.5. Adsorption isotherms

Batch adsorption studies of cesium ions was performed at room temperatures and initial pH of 9.4 to obtain the equilibrium isotherms. A series of experiments were carried out by contacting a fixed amount of adsorbents with 25 mL of Cs ion solution spiked with a prefixed initial activity and have varying concentrations cover the range of 10^{-3} to 10^{-1} mol L^{-1} and agitated for a sufficiently time (∼2 h) required to reach equilibrium. Then, adsorbents were separated by centrifugation and the amount of metal ion retained in the adsorbents, q, was calculated using:

$$q = (C_0 - C_e)\frac{V}{m} \quad (3)$$

where C_0 and C_e are the initial and equilibrium concentration of Cs in aqueous solution. All experimental data were the average of three replications of each experiment and the reproducibility of experimental measurements were mostly within 1 ± 0.72%.

3. Results and discussions

3.1. Adsorbent characterization

The surface area, measured by the N_2-BET method, is 98.24 and 126.6 m^2 g^{-1} for magnetite and iron ferrite, respectively. These high values reveal the existence of a high porosity responsible for the strong capacity of these magnetic materials to fix some cations. A potentiometric titration method was used to

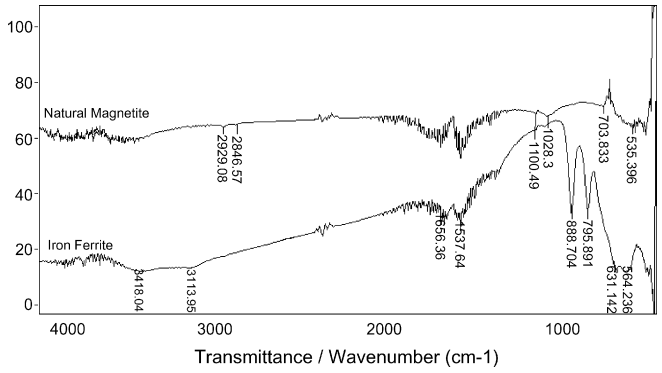

Fig. 1. FTIR spectra of iron ferrite and natural magnetite.

determine the pH corresponding to zero point charge (pH_{zpc}) [15], and found to be around 6.4 and 6.6 for natural magnetite and ferrite, respectively.

The infrared spectra of the synthesized ferrite and natural magnetite are shown in Fig. 1. The spectra show several bands can be categorized into four main absorption ranges at 2800–3400, 1500–1650, 1000–1100 and 500–900 cm^{-1}. The characteristic absorption bands at 2800–3400 cm^{-1} may be related to the strong inter- and intramolecular hydrogen bonding. The absorption bands at 1500–1650 cm^{-1} may be assigned to the interstitial bonded water [16]. The bands arising at 1000–1100 cm^{-1} may be ascribed to Fe–OH vibration interactions while the several bands in the range 500–900 cm^{-1} are indicative to the presence of Fe–O–Fe bond [17].

The thermal analysis of the applied adsorbents was performed in the range 0–600 °C using DTA-TG analysis and the thermograms are illustrated in Figs. 2 and 3. The differential thermal analysis (DTA) of ferrite shows four endothermic peaks at ~60, 226, 259 and 321 °C. These peaks are corresponding to the evaporation of free water molecules and that physically adhered to surface and wall's pores of adsorbents (dehydration). TGA analysis exhibits an overall weight loss, corresponding to the obtained endothermic peaks, only amounted to 8.5% of the initial weight of sample at 600 °C implying high thermal stability up to the applied range of temperature. Also, Fig. 3 clarifies that natural magnetite has

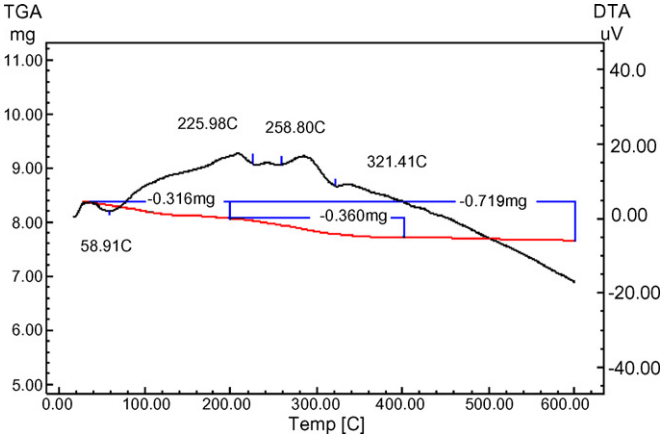

Fig. 2. DTA–TG thermograms of iron ferrite.

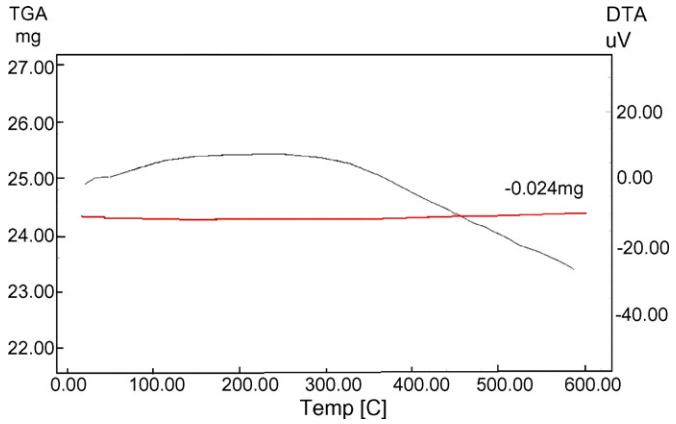

Fig. 3. DTA–TG thermograms of natural magnetite.

an optimum thermal stability with approximately no weight loss.

3.2. Adsorption study

3.2.1. The effect of pH

The effect of pH on the efficiency of cesium adsorption on natural magnetite and iron ferrite is represented in Fig. 4. The results clarify that the distribution coefficient (K_d) generally increases with increasing pH values of solution from 2.4 up to 11. Depending upon solution pH, the oxide surface can act as a weak acid or base and gain or lose proton (i.e. it can undergo protonation or deprotonation) [18,19]. Therefore, the following reactions are expected to occur at the surface of adsorbents:

$$SO^- + H^+ \leftrightharpoons SOH \quad (4)$$

$$SOH + H^+ \leftrightharpoons SOH_2{}^+ \quad (5)$$

where SOH represents a singly protonated oxide site. The above reactions reveal that increasing the concentration of deprotonated surface oxide sites increases the adsorption capacity of cations that proposed to occur according to the following reaction:

$$SO^- + M^{n+} + mH_2O \rightleftharpoons SO\text{–}M(OH)_m^{n-m-1} + mH^+ \quad (6)$$

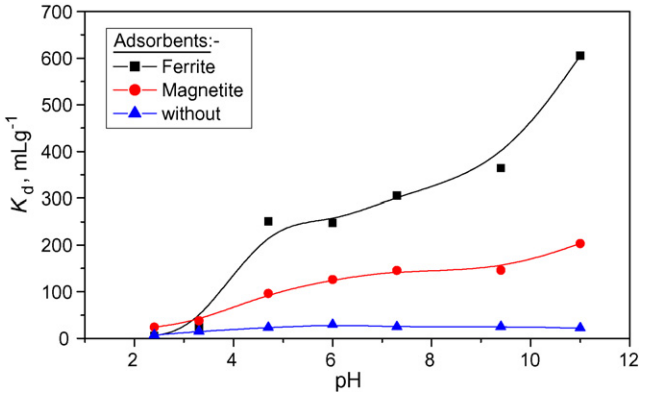

Fig. 4. Variation of distribution coefficient (K_d) of Cs adsorption onto iron ferrite and natural magnetite as a function of pH.

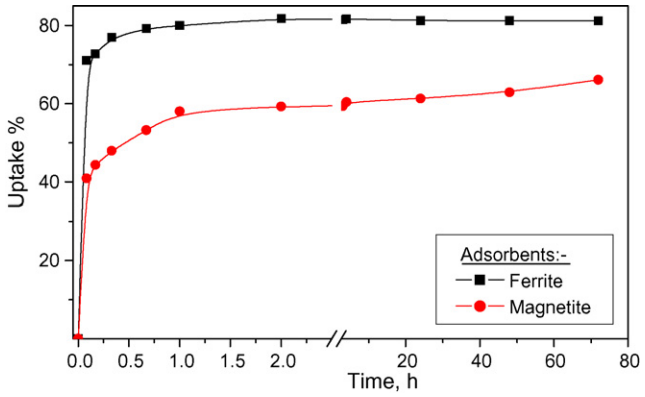

Fig. 5. Effect of equilibrium time on adsorption of Cs onto iron ferrite and and natural magnetite ($V/m = 100$, pH = 9.4, temperature = 23 ± 2 °C).

Sun et al. [20] ruled out that the zeta potential of these magnetic adsorbents at acidic pH is positive and decreases with increasing pH and the corresponding surface reaction may be expressed as:

$$\text{Fe(II, III)OH}_2^+ \overset{\text{H}^+}{\longleftarrow} \text{Fe(II, III)OH} \overset{-\text{H}^+}{\longrightarrow} \text{Fe(II, III)O}^- \quad (7)$$

In acidic pH solution, the dominating surface species is tentatively Fe(II, III)OH_2^+ implying slight Cs adsorption where the electrostatic interactions would be electrically unfavorable in this region. With increasing pH, zeta potential decrease and Fe(II, III)OH becomes the dominating species around pH_{pzc} which is 6.4 and 6.6 for natural magnetite and ferrite, respectively. The removal of Cs from the aqueous solution, at these conditions, may be achieved through an ion exchange process with Fe^{2+} present in adsorbent structure and/or through Cs^+/H^+ exchange according to the following interaction:

$$\text{Fe(II, III)–OH} + \text{Cs}^+ \leftrightharpoons \text{Fe(II, III)–O–Cs} + \text{H}^+ \quad (8)$$

At alkaline pH, the surface species Fe(II, III)O^- is mainly predominant indicating a high Cs adsorption. Through this broad range of initial solution pH values amounted from 2.4 up to 11, the relevant Cs removal is attained at high pH values implying the efficiency of pH adjustment, as a pre-treatment, for removal of Cs from radioactive waste solutions using magnetite sorbents.

3.2.2. The effect of contact time

The effect of contact time on cesium adsorption from aqueous solutions at pH 9.4 is given in Fig. 5. The adsorption percentage increases with shaking time and reveals a rapid removal during the first few minutes of contact, followed by a slow increase until a state of equilibrium is reached. The two steps sorption, the first rapid and quantitatively predominant and the second slower and quantitatively insignificant, has been extensively reported in literature [21]. The rapid step is probably due to the abundant availability of active sites on the material, and with the gradual occupancy of these sites, the sorption becomes less efficient in the slower step. Based on these results, a shaking time of 60 min was assumed to be suitable for subsequent sorption experiments. The uptake percentages attained after equilibrium are 82% and 61% for adsorption onto iron ferrite and natural magnetite, respectively.

In order to investigate the sorption rate law of metal sorption, the kinetic data obtained from batch experiments have been analyzed using the pseudo-second order equation proposed by Ho et al. [22]. The differential equation that describes the pseudo-second order is expressed as:

$$\frac{dq_t}{dt} = k(q_e - q_t)^2 \quad (9)$$

where k is the sorption rate constant (g mg^{-1} h^{-1}), q_e the amount of metal ion adsorbed in the equilibrium (mg g^{-1}) and q_t is the amount of metal ion on the adsorbent surface at any time t (mg g^{-1}). By separating variables and integrating the equation for the initial limits, $t = 0$, $q_t = 0$, the equation:

$$\frac{1}{q_e - q_t} = \frac{1}{q_e} + kt \quad (10)$$

is obtained, which is the integrated rate law for a pseudo-second order reaction and can be rearranged to obtain the following linear form:

$$\frac{t}{q_t} = \frac{1}{kq_e^2} + \frac{1}{q_e}t \quad (11)$$

Thus, by plotting t/qt against t, the values of k, qe and the product kq_e^2 (which represent the rate of the initial adsorption) can be determined graphically from the slope and intercept of the revealed plots. The kinetics plots of t/qt vs. t for Cs adsorption onto iron ferrite and natural magnetite are represented in Fig. 6. The figure exhibits a linear relationship for both adsorbents. This linearity indicates that Cs adsorption ca be approximated with pseudo-second order kinetics and the overall rate-constant appears to be controlled by chemisorption mechanism through sharing or exchange of electrons between adsorbent surface and adsorbate ions [23,24]. The equilibrium metal sorption, qe, the values of the rate constant, k, and the correlation coefficients, R^2, were calculated and are presented in Table 1.

When comparing the obtained values for the sorption capacity, q_e, the calculated values of q_e, using Ho et al. model agree well with the experimental data clarifying the matching of the experimental data to the pseudo-second order kinetics. The rate

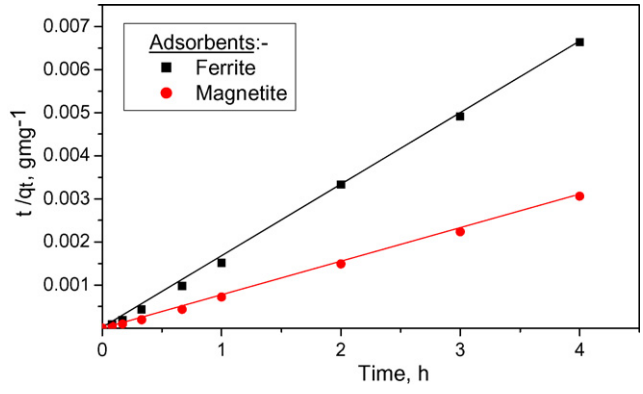

Fig. 6. Pseudo-second order kinetic fit for Cs adsorption onto iron ferrite and natural magnetite ($V/m = 100$, pH = 9.4, temperature = 23 ± 2 °C).

Table 1
Kinetic parameters of pseudo-second order model for Cs adsorption on iron ferrite and natural magnetite

Adsorbent	q_e (mg g^{-1})	k (g mg^{-1} h^{-1})	R^2
Ferrite	114.9	76.83×10^4	1.000
Magnetite	68.49	18.75×10^4	0.999

constant is extremely high and is greater for Cs adsorption on iron ferrite than that on magnetite.

3.2.3. The influence of competing metal ions

The adsorption of Cs on iron ferrite and natural magnetite in presence of competing cations was studied using multivalent metal ions with varying initial concentrations. The variation in adsorption efficiency of Cs^+ versus the initial concentration of Na^+ and Mg^{2+} and Al^{3+} is given in Figs. 7 and 8. It is clearly seen that the selectivity of the applied adsorbents towards cesium ions was seriously affected by presence of competing ions where adsorption percentage decreases with increasing bulk metal concentration in the solutions from 5×10^{-2} up to 4×10^{-1} mol L^{-1}. This could possibly be attributed to the hindrance caused by these interfering cations that exit in much larger quantities than Cs^+ ions and competes with it for the active sites in adsorbents surface.

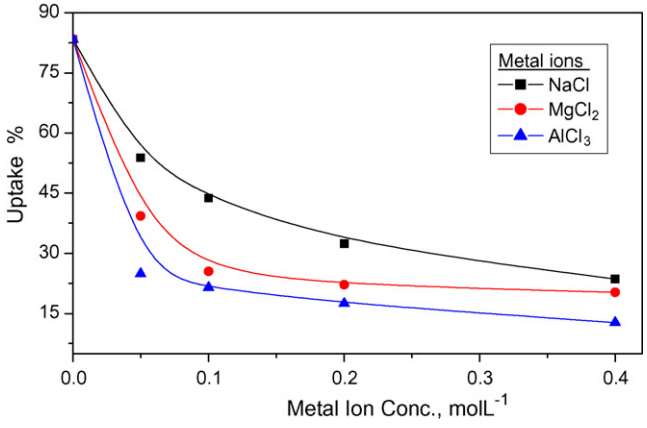

Fig. 7. Effect of interfering cations on adsorption of Cs onto iron ferrite.

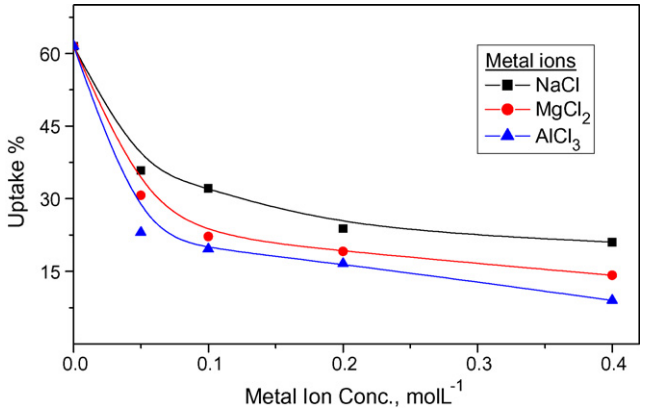

Fig. 8. Effect of interfering cations on adsorption of Cs onto natural magnetite.

3.3. Adsorption isotherms

To optimize the design of an adsorption system for the removal of adsorbates, it is important to establish the most appropriate correlation for the equilibrium curves. In this concern, various isotherm equations have been used to describe the equilibrium nature of adsorption processes in heterogeneous systems. Large numbers of researchers in the field of environmental engineering have used Freundlich and Langmuir isotherm equations to represent equilibrium adsorption data of many systems. This, despite the fact that these equations have serious limitations on their usage, the most popular Freundlich isotherm is suitable for highly heterogeneous surfaces, however, it is valid for adsorption data over a restricted range of concentrations. For highly heterogeneous surfaces and extremely low concentrations, Henry's law is valid. However, Freundlich equation [25] does not approach Henry's law at vanishing concentrations. The Langmuir equation [26], although follows Henry's law at vanishing concentrations, is valid for homogeneous surfaces. Thus, both these isotherm equations may not be suitable for metal ion adsorption on some inorganic resins for the whole range of concentrations used. Temkin isotherm contains a factor that explicitly takes into account the interactions between adsorbing species and the adsorbate. This isotherm assumes that (i) the heat of adsorption of all the molecules in the layer decreases linearly with coverage due to adsorbate–adsorbate interactions and (ii) adsorption is characterized by a uniform distribution of binding energies, up to some maximum binding energy [27,28]. The Dubinin–Radushkevich (D–R) isotherm model is more general than the Langmuir isotherm since it does not assume a homogeneous surface or constant sorption potential. It was applied to distinguish between the physical and chemical adsorption of metal ions [29,30]. The Redlich–Peterson equation is a three parameter-equation, often used to represent solute adsorption data on heterogeneous surfaces [31]. These equations are reduced to Henry's equation at very low concentrations.

In this study, we tried to use the isotherm equations given by Freundlich, Langmuir, Temkin, Dubinin–Radushkevich (D–R) and Redlich–Peterson (R–P) to fit the revealed experimental data for Cs adsorption. The isotherm parameters (two for Freundlich, Langmuir and Temkin, and three for Dubinin–Radushkevich and Redlich–Peterson models) were obtained from the logarithmic form of the isotherms equations.

The Freundlich, Langmuir, Temkin, Dubinin–Radushkevich and Redlich–Peterson equations are expressed, respectively, by:

$$q_e = K_F C_e^{1/n} \tag{12}$$

$$q_e = \frac{Q_m K_L C_e}{1 + K_L C_e} \tag{13}$$

$$q_e = b_T \ln K_T C_e \tag{14}$$

$$q_e = Q_m \exp(-K_D \varepsilon^2) \tag{15}$$

$$q_e = \frac{K_R C_e}{1 + a_R C_e^{\alpha}} \tag{16}$$

where q_e is the amount of cesium ions adsorbed per unit weight of adsorbent at equilibrium (mg g^{-1}), C_e the equilibrium

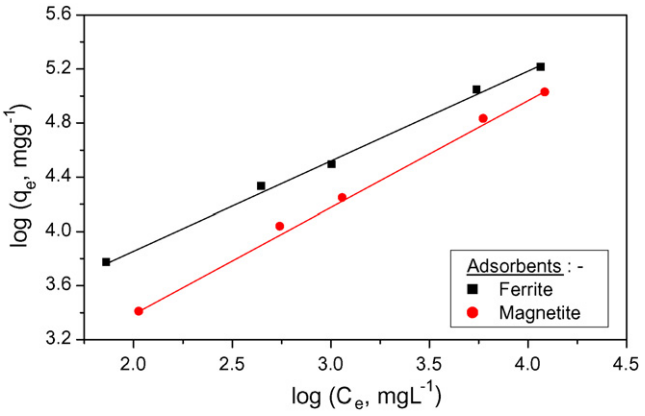

Fig. 9. Freundlich isotherm plots for adsorption of Cs onto iron ferrite and natural magnetite.

concentration of cesium ions in solution (mg L^{-1}), q_m the maximum adsorption capacity of the adsorbent (mg g^{-1}), K_F the constant of Freundlich isotherm (mg$^{(1-1/n)}$ L$^{1/n}$ g^{-1}), $1/n$ the Freundlich isotherm exponent constant related to the adsorption intensity, K_L the constant of Langmuir isotherm indicates monolayer adsorption capacity (L g^{-1}), K_T the constant of Temkin isotherm (L g^{-1}), and b_T is the Temkin isotherm constant related to the heat of adsorption (kJ mol^{-1}). The constant K_D (mol^2 kJ^{-2}) gives the mean free energy E (kJ mol^{-1}) of adsorption per molecule of the sorbate when it is transferred to the surface of the solid from infinity in the solution, ε polanyi potential constant given as $RT\ln(1+1/C_e)$, R the universal gas constant (8.3145 J mol^{-1} K^{-1}), T the absolute temperature (K), K_R, a_R constant of Redlich–Peterson isotherm (L g^{-1}), and α the empirical constant have the values ($0<\alpha<1$).

The concentration dependence in Cs adsorption onto iron ferrite and magnetite has been fitted to the logarithmic form of the above equations and the data revealed are displayed in Figs. 9–13. From the slopes and intercepts of the linear graphs, the different models constants were calculated and their values are given in Table 2.

Freundlich model was chosen to estimate the adsorption intensity of the sorbate ions on the adsorbent surface. The experimental data, plotted logarithmically using the linear Freundlich isotherm equation, are given in Fig. 9 and the isotherm constants are presented in Table 2. The Freundlich isotherm parameter ($1/n$), that measures the adsorption intensity of Cs ions on applied adsorbents, showed values less than unity (0.658 and 0.788) indicating that the isotherms can be characterized by a convex Freundlich isotherm. This implies that a significant adsorption may take place even at high metal ion concentration.

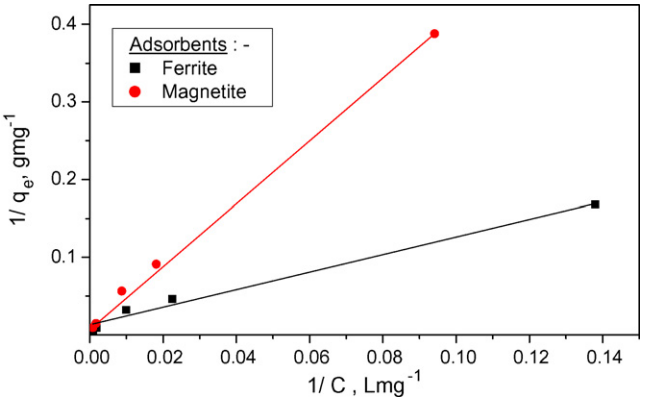

Fig. 10. Langmuir isotherm plots for adsorption of Cs onto iron ferrite and natural magnetite.

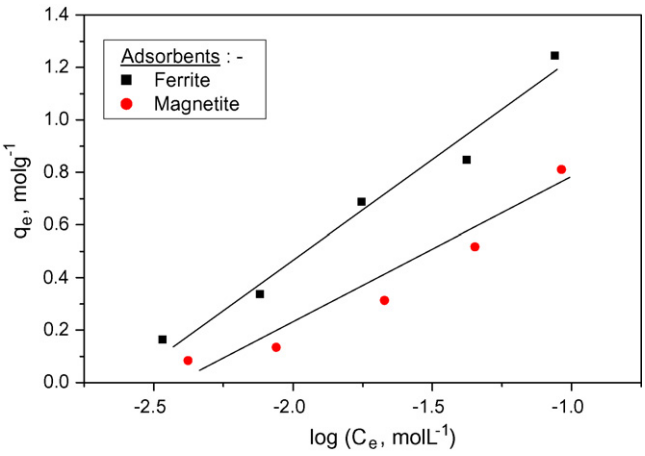

Fig. 11. Temkin isotherm plots for adsorption of Cs onto iron ferrite and natural magnetite.

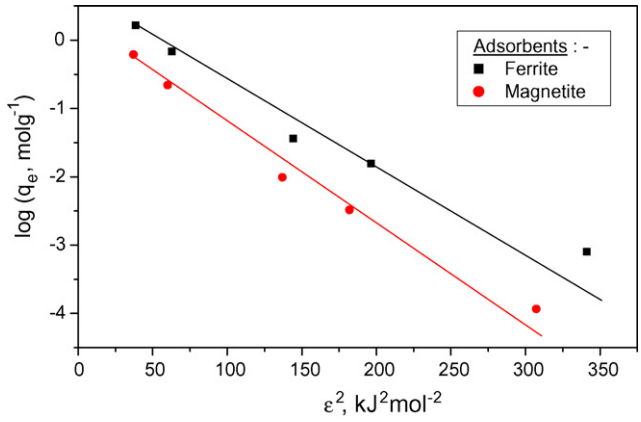

Fig. 12. Dubinin–Radushkevich isotherm plots for adsorption of Cs onto iron ferrite and natural magnetite.

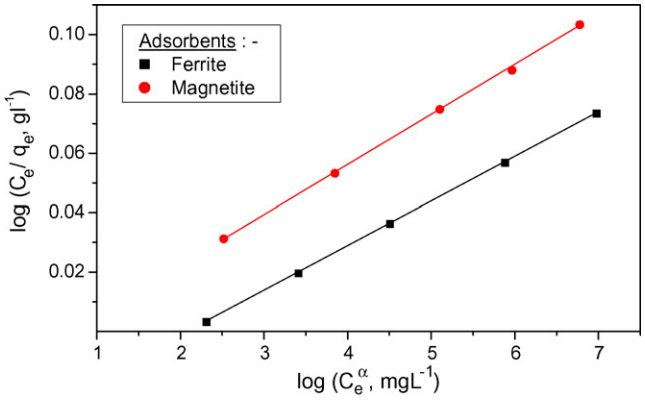

Fig. 13. Redlich–Peterson isotherm plots for adsorption of Cs onto iron ferrite and natural magnetite.

The K_F value ($mg^{(1-1/n)}\,L^{1/n}\,g^{-1}$) of Cs adsorption onto ferrite (36.2) is greater than that for adsorption onto magnetite (6.92), confirming that the prepared iron ferrite has greater adsorption tendency towards the Cs ions than the natural magnetite.

Langmuir isotherm model was chosen for the estimation of maximum adsorption capacity corresponding to complete monolayer coverage on the magnetic adsorbents. The plot of specific Cs adsorption ($1/q_e$) against $1/C_e$ is shown in Fig. 10. The adsorption capacity, Q_m, which is a measure of the maximum sorption capacity corresponding to complete monolayer coverage showed a mass capacity of 108.58 and 70.77 mg g^{-1} for iron ferrite and natural magnetite, respectively. The adsorption coefficient, K_L that is related to the apparent energy of adsorption onto iron ferrite (0.815 L g^{-1}) was greater than that for magnetite (0.353 L g^{-1}). Furthermore, the favorability of adsorption of Cs ions on these magnetic adsorbents was tested using the essential features of the Langmuir isotherm model, expressed in terms of a dimensionless constant called separation factor (S_F) which is defined by the expression [32–34]:

$$S_F = \frac{1}{1 + K_L C_o} \tag{17}$$

The values of this parameter are less than unity indicating that the adsorption is favorable and the used magnetic adsorbents are optimum for removal of Cs ions from waste solutions.

Temkin adsorption isotherm model was applied to evaluate the adsorption potentials of the applied adsorbents for adsorbate ions. The isotherm plot is presented in Fig. 11. The values of Temkin adsorption potential constant (K_T) are 361 and 262 L g^{-1} for adsorption of Cs onto iron ferrite and magnetite, respectively. The value of Temkin constant (b_T) that related to the heat of Cs adsorption onto ferrite and magnetite are estimated to be 0.337 and 0.235 kJ mol^{-1}, respectively. These low values indicates a weak interaction between Cs ions and the adsorbents surface supporting an ion-exchange mechanism to predominate the adsorption process. This evidences reinforces the emphasis stemmed from the role of solution pH that indicates that Cs adsorption is attributable through an ion-exchange process.

The Dubinin–Radushkevich isotherm is the popular model that used to estimate the characteristic porosity and the apparent free energy of adsorption. The linear regression of Dubinin–Radushkevich isotherm plot is presented in Fig. 12 and the isotherm parameters are shown in Table 2. The maximum sorption capacity (Q_m) of the applied adsorbents for Cs ions are found to have the values of 1.55 and 1.13 mol g^{-1} with iron ferrite and natural magnetite. The values of porosity factors (K_D) are 2.19×10^{-5} and 2.57×10^{-5} $mol^2\,kJ^{-2}$, respectively. These values are less than unity and so imply the adsorbents to have fine micropores and indicate a surface heterogeneity may be arisen from the pore structure as well as adsorbate–adsorbent interactions [35]. The mean energy of adsorption (E, kJ mol^{-1}), which is the free energy change when 1 mol of ion is transferred to the surface of the solid from infinity in the solution, was calculated using the relationship [36,37]:

$$E = (-2K_D)^{-1/2} \tag{18}$$

The apparent free energies estimated from the Dubinin–Radushkevich model parameters are 32.29 and 27.51 kJ mol^{-1} for Cs adsorption onto iron ferrite and natural magnetite, respectively. These estimated energy values are comparable to that of general ion exchange or chemisorption that amounted to 40 kJ mol^{-1} [38]. Therefore, it was expected that Cs ions are removed from aqueous solutions through an ion exchange interaction with the oxide ions on adsorbent surface. The positive values indicate that the sorption process is endothermic in nature.

The three parameter isotherm model given by Redlich and Peterson was applied to represent Cs adsorption data under surface heterogeneity conditions that revealed from Dubinin–Radushkevich isotherm model. The linear regression of Redlich–Peterson isotherm plot is presented in Fig. 13. The values of Redlich–Peterson adsorption constant K_R are 31.5 and 87.7 L g^{-1} for adsorption of Cs onto iron ferrite and natural magnetite, respectively, while that of a_R are 0.47 and 1.44 L g^{-1}. The empirical constant (α) has the values 0.29 and 0.22 for adsorption on iron ferrite and natural magnetite.

The ultimate sorption capacity of both iron ferrite and natural magnetite calculated from the modeled isotherm data is illustrated in Table 3. The data clarify that there are no significant differences between experimental and modeled values

Table 2
Estimated isotherm model constants for Cs adsorption onto iron ferrite and natural magnetite

Isotherm	Adsorbent	Model parameters			
		$1/n$	K_F ($mg^{(1-1/n)}\,L^{1/n}\,g^{-1}$)	R^2	S.D.
Freundlich	Ferrite	0.658	36.2	0.998	0.036
	Magnetite	0.788	6.96	0.997	0.034

Isotherm	Adsorbent	Model parameters			
		Q_m (mg g^{-1})	K_L (L g^{-1})	R^2	S_F
Langmuir	Ferrite	108.58	0.815	0.993	0.271
	Magnetite	70.77	0.353	0.999	0.462

Isotherm	Adsorbent	Model parameters			
		b_T (kJ mol^{-1})	K_T (L g^{-1})	R^2	S.D.
Temkin	Ferrite	0.337	361	0.980	0.120
	Magnetite	0.235	262	0.978	0.087

Isotherm	Adsorbent	Model parameters			
		Q_m (mol g^{-1})	K_D ($mol^2\,kJ^{-2}$)	R^2	E (kJ mol^{-1})
Dubinin – Radushkevich	Ferrite	1.55	2.19×10^{-5}	0.987	32.29
	Magnetite	1.13	2.57×10^{-5}	0.992	27.51

Isotherm	Adsorbent	Model parameters			
		α	K_R (L g^{-1})	a_R (L g^{-1})	R^2
Redlich–Peterson	Ferrite	0.29	31.5	0.47	0.999
	Magnetite	0.22	87.7	1.44	0.999

V/m = 100, pH = 9.4, temperature = 23 ± 2 °C, time = 24 h.

Table 3
The experimental and modeled values of sorption capacity of the magnetic adsorbents towards Cs(I) ions

Adsorbent	Q_m (experimental)		Q_m (modeled)		
	mg g^{-1}	mol g^{-1}	Ho et al. (mg g^{-1})	Langmuir (mg g^{-1})	D–R (mol g^{-1})
Ferrite	111.72	0.847	114.9	108.58	1.55
Magnetite	68.28	0.517	68.49	70.77	1.13

of the sorption capacity of both adsorbents. This indicates that the different isotherm models are appropriate in their merits in describing the potential of the magnetic adsorbents for the removal of Cs ions from hazardous wastes. Based on the correlation coefficient of determination (R^2), the three parameters Redlich–Peterson adsorption isotherm model mostly provide a better fit of our experimental data while the other isotherm models produce a satisfactorily fit. Generally, the analysis of experimental results by equilibrium sorption isotherms is important in developing accurate data that could be used for sorption design purposes. The sorption equation parameters and the underlying thermodynamic assumptions of these equilibrium models often provide some insight into both the sorption mechanism and the surface properties and affinity of the adsorbent.

4. Conclusion

We have prepared iron ferrite and applied it, with natural magnetite, in batch adsorber for removal of Cs from waste solutions. The synthesized adsorbent compared with the natural one, exhibits satisfactory characteristics to be included in treatment of hazardous wastes and separation of valuable elements, especially some fission products from active wastes. It has good thermal stability and high sorption capacity. The quantitative removal of Cs was highly attained from basic solutions implying the efficiency of pH adjustment, as a pre-treatment, for removal of Cs from radioactive waste solutions using magnetite sorbents. The adsorption process follows a pseudo-second order kinetics and its efficiency was depressed by presence of interfering cations. The equilibrium adsorption data are satisfactorily fitted to five isotherm models are Freundlich, Langmuir, Temkin, Dubinin–Radushkevich and Redlich–Peterson that best correlate the experimental data. Based on the models parameters, Cs adsorption onto both ferrite and magnetite was suggested to an endothermic process controlled by ion-exchange mechanism. The proposed adsorbent shows high affinity to Cs ions that retained on adsorbent surface via a favorable adsorption.

References

[1] P.J. Coughtrey, M.C. Thorne, Radionuclide Distribution and Transport in Terrestrial and Aquatic Ecosystems, vol. 2, A.A. Balkema, Rotterdam, 1983.
[2] G. Gűrboğa, H. Tel, Y. Altaş, Sep. Purif. Technol. 47 (2006) 96.
[3] IAEA, Remediation of Areas Contaminated by Past Activities and Accidents, Safety Requirements, Safety Standards Series No. WSR-3, STI/PUB/1176, IAEA, Austria, 2003.
[4] T. Moller, A. Clearfield, R. Harjula, Micropor. Mesopor. Mater. 54 (2002) 187.
[5] S.P. Mishra, D. Tiwary, Appl. Radiat. Isotopes 51 (1999) 359.
[6] V. Efremenkov, E. Hooper, V Kourim (Eds.), Use of Inorganic Sorbents for Treatment of Liquid Wastes and Backfill Backfill of Underground Repositories, IAEA-TECDOC-675, IAEA, Vienna, 1992.
[7] A. Ruvarac, in: A. Clearfield (Ed.), Inorganic Ion Exchange Materials, CRC Press Inc., Boca Raton, FL, 1982.
[8] Y.K. Kim, K.J. Lee, J. Nucl. Sci. Technol. 38 (9) (2001) 785.
[9] T.E. Boyd, Radioact. Waste Manage. Nucl. Fuel Cycle 4 (2) (1983) 195.
[10] J.H. Cheong, K.J. Lee, Sep. Sci. Technol. 31 (1996) 1137.
[11] R.L. Kochen, J.D. Navratil, US Patent 5,595,666 (1997).
[12] J.D. Navratil, Australian Patent Application PJ0198 (1998).
[13] M.H. Liao, D.H. Chen, Chem. Lett. 32 (2003) 488.
[14] S.Y. Mak, D.H. Chen, Dyes Pigments 61 (2004) 93.
[15] H.H. Someda, M.R. Ezz El-Din, R.R. Sheha, H.A. El-Naggar, J. Radioanal. Nucl. Chem. 254 (2) (2002) 373.
[16] R.N. Nyquist, R.O. Kagel, Infrared and Raman Spectra of Inorganic Compounds and Organic Salts, Academic Press Inc., 1997.
[17] K. Nakamoto, Infrared and Raman Spectra of Inorganic and Coordination Compounds and Organic Salts, John Wiley & Sons Publications, New York, 1978.
[18] M.M. Benjamin, K.F. Hayes, J.O. Leckie, J. Water Poll. Control Fed. 54 (11) (1982) 1472.
[19] K. Banerjee, Cases studies for immobilizing toxic metals with iron coprecipitation and adsorption, in: A.K. SenGupta (Ed.), Environmental Separation of Heavy Metals: Engineering processes, CRC Press LLC, Washington, 2002, p. 181.
[20] Z.X. Sun, F.W. Su, W. Forsling, P.O. Samskog, J. Colloid Interf. Sci. 197 (1998) 151.
[21] Y. Sag, T. Kutsal, Process Biochem. 31 (1996) 561.
[22] Y.S. Ho, W.T. Chiu, C.S. Hsu, C.T. Huang, Hydrometallurgy 73 (2004) 55.
[23] V.C. Taty-Costades, H. Fauduest, C. Porte, A. Delacroix, J. Harzard. Mater. B 105 (2003) 121.
[24] Y.S. Ho, G. McKay, Process Biochem. 34 (1999) 451.
[25] H.M.F. Freundlich, J. Phys. Chem. A 57 (1906) 385.
[26] I. Langmuir, J. Am. Chem. Soc. 40 (1918) 1361.
[27] M.I. Temkin, V. Pyzhev, Acta Physiochim. URSS 12 (1940) 327.
[28] Y. Kim, C. Kim, I. Choi, S. Rengraj, J. Yi, Environ. Sci. Technol. 38 (2004) 924.
[29] S.H. Lin, R.S. Juang, J. Hazard. Mater. 92 (2002) 315.
[30] M.M. Dubinin, L.V. Radushkevich, Proc. Acad. Sci. Phys. Chem. Sec., U.S.S.R. 55 (1947) 331.
[31] O. Redlich, D.L. Peterson, J. Phys. Chem. 63 (1959) 1024.
[32] K.R. Hall, L.C. Eagleton, A. Acrivos, T. Vermeulen, Ind. Eng. Chem. Fundam. 5 (1966) 212.
[33] R.S. Juang, F.C. Wu, R.L. Tseng, Environ. Technol. 18 (1997) 535.
[34] S.S. Gupta, K.G. Bhattacharyya, J. Colloid Interf. Sci. 295 (2006) 21.
[35] B.T. Kim, H.K. Lee, H. Moon, K.J. Lee, Sep. Sci. Technol. 30 (16) (1995) 3165.
[36] S.M. Hasany, M.H. Chaudhary, Appl. Radiat. Isotopes 47 (1996) 467.
[37] A. Benhammoua, A. Yaacoubi, L. Nibou, B. Tanouti, J. Colloid Interf. Sci. 282 (2005) 320.
[38] F. Helfferich, Ion Exchange, McGraw-Hill, NY, 1962.